

Multi Story Semi-Active Tuned Mass Damper Building System

SUMMARY

To overcome the inability of the Tuned Mass Damper (TMD) system, which has linear properties and limitations on the weight, this paper suggests a multi story Semi-Active Tuned Mass Damper (SATMD) building system using a structure's upper portion as the tuned mass damper and resettable actuator as a semi-active (SA) control device. For this purpose, it is proposed to segregate the building's upper story(s) with rubber bearings, and employ SA resettable actuator and viscous damper to the story(s) of upper segment to lower structural elements. The optimal frequency tuning ratio and damping ratio is considered for large mass ratio, for which previously proposed equation was used and the practical optimal stiffness was allocated to the actuator stiffness and rubber bearing stiffness. 2DOF model, including SATMD, is adopted to verify the principal efficacy of the suggested structural control concept and 6 and 12 story moment resisting benchmark frames are investigated to assess the viability and effectiveness of the system that aims at reducing the response of buildings to earthquakes. This research determines the feasibility, design methods and effectiveness of the proposed multi story SATMD building system by numerically analyzing and comparing the response with no control and passive TMD system.

1. INTRODUCTION

For flexible structures such as tall buildings, one of the classical dynamic vibrations damping device is the Tuned Mass Damper system. However, it is difficult to draw general conclusions explaining the effectiveness of the TMD for the structures including inelastic behavior due to the great variety of possible inelastic models [4]. In some cases, the specified TMD produced a negative effect, i.e. it amplifies the response slightly. This poor performance is attributed to the ineffectiveness of the TMD, which has only linear properties and its inability to reach a resonant condition in the inelastic structure. It is also found, it requires a relatively large mass, and therefore, a large space for its installation and the corresponding clearance to accommodate such large displacements.

In order to overcome the disadvantages of a TMD system, some ideas have been suggested by using a portion of the building itself as a mass damper. In particular, one idea is to use the building's top story as an absorber's mass. The concept of 'expendable top story' introduced by Jagadish et al. [10] or the 'energy absorbing story' presented by Miyama [13] is an effective alternative where the top story acts as a vibration absorber for the other stories of the building. Another proposal is to convert a mega-structural system to a mega-sub-control system in which exhibits structural efficiency by allowing high rigidity of the system while keeping a minimum amount of structural materials [6]. Murakami et al. [11] described an example of the design of a multifunctional 14-story building including apartments, office rooms, shops and parking lots where a seismic isolation system is installed on the middle-story. Villaverde et al. [17] suggested that 13-story building to assess the viability and effectiveness of a roof isolation system that aims at reducing the response of buildings to earthquakes. It was found that the proposed scheme to build a vibration absorber with a building's roof is effective, and has the potential to

become an attractive way by which to reduce structural and nonstructural earthquake damage in those buildings in which roof weight is a significant percentage of their total weight, that is, low- and medium-rise buildings. Pan and Cui [14] and Pan et al. [15] sought to evaluate the effect of using segmental structures where isolation devices are placed at various heights in the structure, as well as at the base, in order to reduce the displacements imposed on each of the devices. Each segment may comprise a few stories and is interconnected by additional vibrational isolation systems.

For the SA control strategies, Barroso et al. [2] and Hunt [8] presented an investigation of the ability of SA control methods utilizing resettable devices to mitigate structural response in the presence of hysteretic, geometric and yielding nonlinearities under various intensity level seismic hazard suites to define control efficacy and seismic hazard statistics. Jabaari and Bobrow [9] focused on the basic analytical techniques needed to characterize structural systems that use a resettable SA device for vibration suppression. They presented experimental results on the mathematical characterization of the device, and have presented both experimental and simulation results that demonstrate the performance of the device for structural vibration suppression. Yang et al. [20] suggested that a general resetting control law based on the Lyapunov theory for a resetting SA damper and compared with a switching control method through extensive numerical simulations using different types of earthquake excitations. Yang and Agrawal [19] presented the safety performances of various types of hybrid control systems, which consist of the base isolation system and resetting SA dampers for nonlinear buildings against near-field earthquakes. Djajakesukma et al. [5] reported SA stiffness damper system with various control laws, such as resetting control, switching control, LQR and modified LQR and the results were compared with no control and passive control cases. Harovat et al. introduced a concept in structural control of SATMD [7]. In their paper, the SA performance

was found to be very similar to the fully active one, and, in some aspect (e.g., TMD stroke requirements), slightly superior to the active system to wind induced vibrations in tall buildings. Abe [1] also, presented the performance of SATMD with initial TMD displacement and variable damping subject to earthquake excitation. He founded that the SATMD give higher reduction of structural response than conventional passive TMD. Furthermore, although increasing the initial TMD displacement generally reduces the structural response, extremely large TMD displacement does not necessarily give better performance.

In this paper, multi story tuned mass damper building system is suggested and resettable actuator was used as a SA structural control device. For this study, the dynamic characteristics and seismic linear elastic response of the 2DOF model are investigated and two numerical benchmarking model results are compared with those from the corresponding passive tuned mass damper system.

2. STRUCTURAL CONTROL CONCEPT

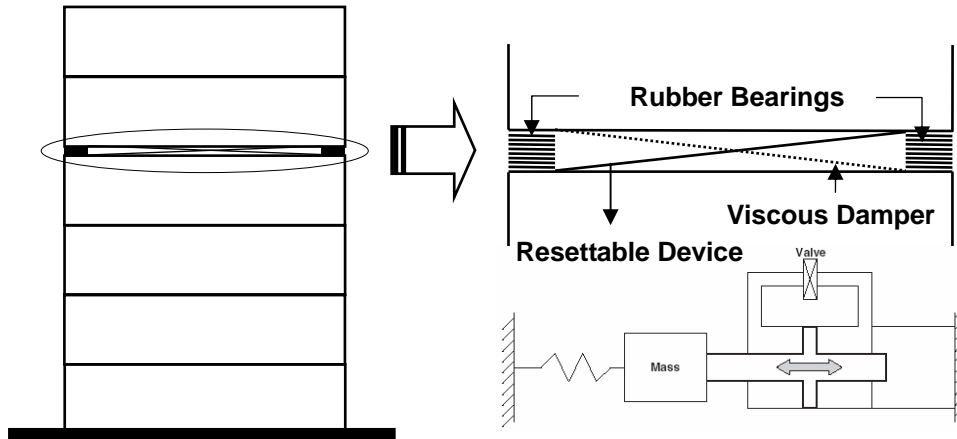


Figure 1. Schematic of suggested model concept and resettable actuator

2.1. Multi story isolation

In an effort to overcome the disadvantages of the Passive Tuned Mass Damper (PTMD) system, such as relatively large mass, large space for their installation and large relative displacements of TMD, the idea of using an upper portion of a building as the mass of the absorber is suggested. This concept can be viewed as an extension of the conventional TMD system. Due to the fact of the large mass ratio of the TMD system, the upper story(s) may experience large displacements, so the upper story(s) should have sufficient strength and ductility to account for large displacements. However, there is no need for the use of restraints to avoid excessive lateral motion or stroke of the tuned mass, since the upper story(s) can be interconnected by the combined isolation system of SA resettable device, rubber bearings, and viscous damper as

depicted in Figure 1. Absorption and dissipation of earthquake input energy are afforded by the isolation part in the upper story(s), so the seismic force of the entire building can be reduced by the isolated story(s) tuned system and the entire building can offer excellent earthquake resisting performances.

2.2. Semi-active resettable actuator

The first peak in the response history of the system with TMD cannot be easily reduced because the TMD passively responds to the structural movement and then mitigates the response of the structure by vibrating out-of-phase with the structural movement. For these reasons, the advantage of the resetting approach providing resisting force which is always at its maximum value and the properties of the number of times extracted energy is higher in the resetting technique, leading to faster and more effective vibration suppression, which can be suggested to be used by adopting modified SATMD system using resettable actuator.

Resettable actuators are essentially pneumatic spring elements in which the un-stretched spring length can be reset to obtain maximum energy dissipation from the structural system. Figure 1 shows schematic of a resettable actuator attached to a one-degree of freedom spring-mass system, where k_1 is the structural stiffness and the attached mass is the structural mass of the main system. The actuator consists of a cylinder-piston system with a valve in the by-pass pipe connecting two sides of the cylinder as shown in Figure 1. With the actuator valve closed, as the actuator is either compressed or extended, energy is stored within the actuator's bi-directional piston-cylinder arrangement and the actuator serves as a stiffness element in which the stiffness

is provided by the bulk modulus of the air in the cylinder. Meanwhile, at the point when the energy storage rate is stationary, the valve between the two cylinder halves is opened and then re-closed, rapidly releasing the energy from the system before it is returned to the structure, with attainable forces dependent on the piston area, piston stroke, and pneumatic bulk modulus. When the instants of opening valve, the piston is free to move and the actuator provides only a small damping without stiffness. Such a stiffness damper can be operated in resetting mode. When the building frame implemented with the proposed SATMD system, the story of upper portion is mounted on rubber bearings that are attached to the inferior face of the story plate and to lower plates attached to the top of the main frame's columns. In addition, the piston of the resettable actuator can be connected to the plate of the upper story, whereas the cylinder is connected to the lower beam of the main frame as shown in Figure 1.

2.3. Control law description

The control law for the resettable actuator is dependent on the rate of energy storage, with the free length of the pneumatic spring reset when the energy storage is maximised. The energy in a single actuator, U_{act} , is given by :

$$U_{act} = \frac{1}{2}k_{act}(v - v_0)^2 \quad (1)$$

where v is the relative displacement of the actuator ends, v_0 is the free length of the pneumatic spring which is at the last reset position, and k_{act} is the effective spring stiffness of the resettable actuator.

As the idea of control law is to remove energy from the structural system as quickly as possible, the control law waits until the energy in the pneumatic spring is maximised, thus dissipating maximum packets of energy before re-applying the control force. Discarding maximum packets of energy is advantageous, as it then minimises the actuator valve-open time during which the actuator applies no control force to the structure. Taking the time derivative of Equation (1), the rate of change of energy is given as :

$$\dot{U}_{act} = k_{act} \dot{v}(v - v_0) \quad (2)$$

where \dot{v} is the relative velocity of the actuator ends, and other variables are as defined for Equation (1). From Equation (2) the control logic can be achieved, as the energy stored in the actuator is stationary when $\dot{U}_{act} = 0$, giving the trivial case of minimum energy storage when $(v - v_0) = 0$, and maximum energy storage when $\dot{v} = 0$. As it is unlikely that the relative velocity will exactly equal zero at the iteration time step, a more robust method of detection was used. As the sign of the velocity values at time steps before and after the stationary point will be different, a simple sign comparison will effectively detect the stationary point. The control law can then be written as $v_0 = v$ whenever $\text{sgn}(\dot{v}_t) \neq \text{sgn}(\dot{v}_{t-1})$.

Where the subscripts (t) and (t-1) represent current and previous time steps respectively. The control force applied to the structure for an actuator, u , is then simply that of a displaced spring with the additional logic incorporating actuator saturation :

$$\begin{aligned} u &= -k_{act}(v - v_0) \quad \text{if } u < F_{\max} \\ u &= -F_{\max} \text{sgn}(v - v_0) \quad \text{if } u > F_{\max} \end{aligned} \quad (3)$$

where F_{\max} is the actuator saturation force. It should be noted that the displacement of the

actuator, v , is measured relative to the time-varying dynamic equilibrium point. The inclusion of the structure's yielded position during strong motions reduces the likelihood of the actuator forces attempting to re-yield the structure back to its original static position, which would result in increased structural damage.

The purpose of this paper is to study the seismic effectiveness of a new concept of a multi story semi-active tuned mass damper (SATMD) building system by using the above combined approaches using the building's upper story(s) for the large tuned mass ratio and the SA-active resettable actuator as a SA controller device.

3. SATMD MODEL CONFIGURATIONS

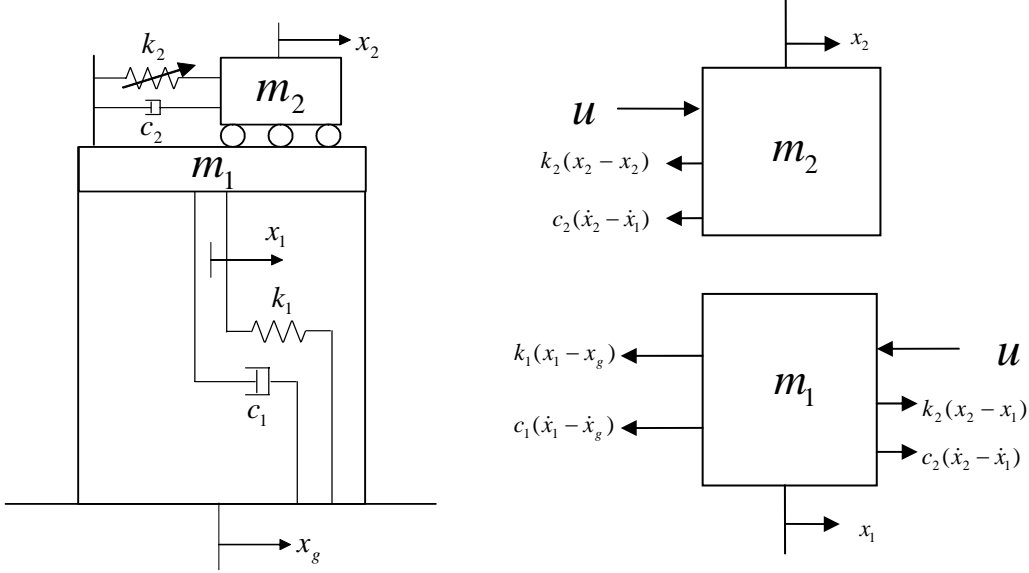


Figure 2. Main System with SATMD and Free Body Diagram

From the 2DOF model for the analysis of main system with a SATMD, the equation of motion of the system subjected to the earthquake load \ddot{x}_g can be derived in the form of

$$\begin{aligned} m_1 \ddot{x}_1 &= -k_1(x_1 - x_g) - c_1(\dot{x}_1 - \dot{x}_g) + k_2(x_2 - x_1) + c_2(\dot{x}_2 - \dot{x}_1) - u \\ m_2 \ddot{x}_2 &= -k_2(x_2 - x_1) - c_2(\dot{x}_2 - \dot{x}_1) + u \end{aligned} \quad (4)$$

The equations can be rearranged in matrix form in terms of the absolute and relative displacements respectively as follows :

$$\begin{bmatrix} m_1 & 0 \\ 0 & m_2 \end{bmatrix} \begin{Bmatrix} \ddot{x}_1 \\ \ddot{x}_2 \end{Bmatrix} + \begin{bmatrix} c_1 + c_2 & -c_2 \\ -c_2 & c_2 \end{bmatrix} \begin{Bmatrix} \dot{x}_1 \\ \dot{x}_2 \end{Bmatrix} + \begin{bmatrix} k_1 + k_2 & -k_2 \\ -k_2 & k_2 \end{bmatrix} \begin{Bmatrix} x_1 \\ x_2 \end{Bmatrix} = \begin{Bmatrix} -1 \\ 1 \end{Bmatrix} u + \begin{Bmatrix} k_1 \\ 0 \end{Bmatrix} x_g + \begin{Bmatrix} c_1 \\ 0 \end{Bmatrix} \dot{x}_g \quad (5)$$

$$\begin{bmatrix} m_1 & 0 \\ m_2 & m_2 \end{bmatrix} \begin{Bmatrix} \ddot{y}_1 \\ \ddot{y}_2 \end{Bmatrix} + \begin{bmatrix} c_1 & -c_2 \\ 0 & c_2 \end{bmatrix} \begin{Bmatrix} \dot{y}_1 \\ \dot{y}_2 \end{Bmatrix} + \begin{bmatrix} k_1 & -k_2 \\ 0 & k_2 \end{bmatrix} \begin{Bmatrix} y_1 \\ y_2 \end{Bmatrix} = \begin{Bmatrix} -1 \\ 1 \end{Bmatrix} u + \begin{Bmatrix} -m_1 \\ -m_2 \end{Bmatrix} \ddot{x}_g \quad (6)$$

Also, the following notations can be used in cases:

- $y_1 = x_1 - x_g$ relative displacement between the main system and the ground
- $y_2 = x_2 - x_1$ relative displacement between the SATMD and the main system
- $\ddot{x}_1 = \ddot{x}_g + \ddot{y}_1$ absolute acceleration of the main system
- $\ddot{x}_2 = \ddot{x}_g + \ddot{y}_1 + \ddot{y}_2$ absolute acceleration of the SATMD

3.1. Parametric optimization

The performance of TMD systems in buildings and other structures can be readily assessed by parametric studies. In general, the optimal parameters such as the frequency tuning ratio and damping ratio of the TMD need to be determined to achieve the optimal performance. Numerous studies on the applicability of TMD for seismic applications were carried out by Villaverde[18], where it was found that TMD performed best when the first two complex modes of vibration of the combined structure and damper, have approximately the same damping ratios, as the average of the damping ratios of the structure and the TMD, as defined:

$$(\xi_1 + \xi_2)/2 \quad (7)$$

To achieve this, it was shown analytically that the TMD should be in resonance with the main structure ($f = 1$) and its damping ratio should satisfy equation is given by:

$$\xi_2 = \xi_1 + \Phi \sqrt{\mu} \quad (8)$$

where Φ is the amplitude of the mode shape at the TMD location. Numerical results, however, show that such formulation does not result in equal dampings in the first modes of vibration, especially for large mass ratios .

To solve the problem of larger mass ratio, larger than 0.005, Sadek et al. [30] proposed another procedure to achieve equal damping in the two vibration modes. They found that the optimum values are determined when the difference between each of the two damping ratios is the smallest and that the optimum TMD parameters result in approximately equal damping ratios greater than $(\xi_1 + \xi_2)/2$ and equal modal frequencies. The procedure was used for systems with damping ratios $\xi_1=0, 0.02, 0.05$ and mass ratios μ between 0.005 and 0.15. For design purpose, Sadek et al. presented the optimum TMD parameters by simple equations using curve fitting method. Meanwhile, Miranda [30] presented a theoretically approximate model for 2DOFs mechanical systems formulated based on their modal kinetic and modal strain energy. The model was subsequently used to determine optimum parameters that maximize the modal damping of TMDs to be placed at the upper level of buildings with an iterative procedure. Using selected range of mass ratio values, it was shown that the model is capable of closely matching exact numerical results previously obtained by Sadek et al. and that the conclusions previously reached continue to hold valid for mass ratios of up to 100.

In this study, for large mass ratios, the equations from Sadek et al. are used to find the optimal parameters of tuning and damping ratio. For higher values of μ , it is likely that the upper story(s) mass will not be an appendage added to the structure, but a portion of the structure itself as schematically shown in Figure 2. According to the paper of Sadek et al., the equation of the optimal frequency tuning ratio, f_{2opt} , and the optimal damping ratio, ξ_{2opt} , of the TMD system is as follow and these equations result in maximum error of approximately 0.2% in f_2 and 0.4% in ξ_2 respectively.

$$f_{2opt} = \frac{1}{1+\mu} \left(1 - \xi_1 \sqrt{\frac{\mu}{1+\mu}} \right) \quad (9)$$

$$\xi_{2opt} = \frac{\xi_1}{1+\mu} + \sqrt{\frac{\mu}{1+\mu}} \quad (10)$$

For practical application to a real system, it is necessary to obtain applicable parameters for the TMD such as the optimal TMD damping stiffness, k_{2opt} and optimal damping coefficient, c_{2opt} . These parameters can be derived using the parametric relationships between the above optimal parameters derived as follow:

$$k_{2opt} = m_2 \omega_1^2 f_{2opt}^2 = \frac{m_2 \omega_1^2 \left(\xi_1 \sqrt{\frac{\mu}{1+\mu}} - 1 \right)^2}{(1+\mu)^2} \quad (11)$$

$$c_{2opt} = 2m_2 \xi_2 \omega_1 f_{2opt} = \frac{2m_2 \omega_1 \left(1 - \xi_1 \sqrt{\frac{\mu}{1+\mu}} \right) \left(\frac{\xi_1}{1+\mu} - \sqrt{\frac{\mu}{1+\mu}} \right)}{1+\mu} \quad (12)$$

In order to generalize the results, the following non-dimensional parameters are defined:

$$\omega_i^2 = \frac{k_i}{m_i} \quad (i=1,2), \quad c_i = 2\xi_i \omega_i m_i \quad (i=1,2), \quad \mu = \frac{m_2}{m_1}, \quad f_2 = \frac{\omega_2}{\omega_1} \quad (13)$$

Item	Main System	Main+SATMD	Unit
Weight	268	348	kN
1 st Modal Mass	27.3	35.5	kN-s ² /m
Frequency	0.54	0.47	Hz
Stiffness	311	309	kN/m
Natural Period	1.86	2.13	sec

Table 1. Dynamic properties of 2DOF model

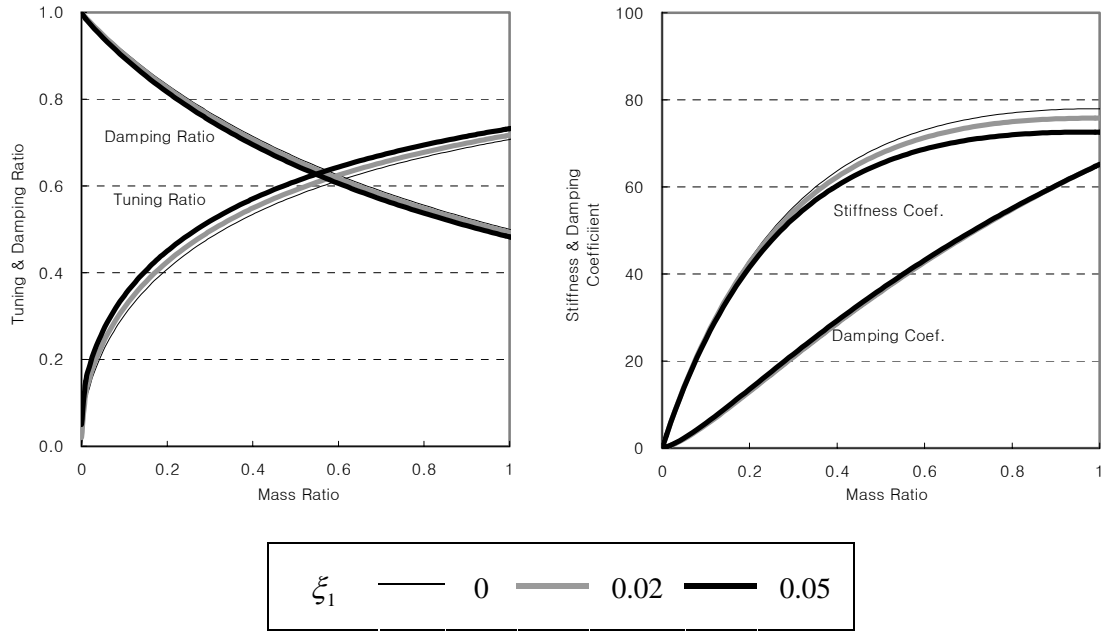


Figure 3. Optimum SATMD parameters VS. mass ratio

Applying the above Sadek et al.'s equations and suggested to the model of 2DOF (as shown in Table) with three different critical damping ratios, $\xi_1=0, 0.02$ and 0.05 , the optimal parameters f_{2opt} , ξ_{2opt} , k_{2opt} , and c_{2opt} for different mass ratios, varying from 0.0 to 1.0 were depicted in Figure 3. It is evident that increasing μ , requires a decrease in f_{2opt} , and an increase in ξ_{2opt} , thus resulting in a higher damping in the modes of vibration. The higher the damping ratio of the structure, ξ_1 , the lower is the f_{2opt} , and higher is the ξ_{2opt} . Figure 3 may be used to select the TMD parameters by estimating its mass, computing the mass ratio μ , and then determining the f_{2opt} and ξ_{2opt} . According to the Equation (11) and (12), the optimal TMD stiffness, k_{2opt} , and damping coefficient, c_{2opt} , for different mass ratios, from 0.0 to 1.0 were also plotted in Figure 3.

3.2. Modeling of SATMD

To represent the effects of the SATMD rubber bearing stiffness coefficient, the spring member that is incorporated to the inelastic dynamic analysis program, *RUAUMOKO 2D* [3] was used. In *RUAUMOKO 2D*, this member may be used to model special effects in the structure or to represent members acting out of the plane of the frame but representing forces that act in the plane of the frame. Figure 4 shows the model structure of the spring member. An optimal SATMD stiffness, k_{2opt} which was obtained from the parametric study of Sadek et al. can be applied to the sum value of the stiffness of the SA device and rubber bearing elements in the transverse direction.

The other component, the SATMD damping which may be added to a structure, can be modeled using the damping or dash-pot member in the program *RUAUMOKO* as shown in Figure 4. This model represents the action of a local viscous energy dissipator that may exist in the structure and contribute to the damping matrix of the structure. An optimal SATMD damping coefficient, c_{2opt} , can be used as the transverse damping coefficient. For the hysteresis rule for the spring member and the damper member, a linear elastic hysteresis has been used to represent the elastic properties of its behaviour. The spring stiffness and the damping coefficient are the important factors which affect the properties of the SATMD system, as does the mass of the SATMD itself. Furthermore, from the point of view of the structure, the critical damping of the framed structure is another variable which affects the response of the structure with the SATMD.

The hystereses in Figure 5 are the two examples for the SA device force representing the behaviors of the resettable device member. For the saturable case, the force is proportional to the displacement until a saturation force is attained, F_{y+} or F_{y-} (the yield forces for the member)

when the system appears to show a perfectly plastic response. On any reversal of displacement the force is automatically reset to zero, the origin is moves to the existing displacement, and the system will then behave as an elastic member until either saturation is achieved or the displacement again changes sign. The other hysteresis in Figure 5 is an example of unsaturable force case when the maximum device force of 15kN/m is applied. It can be seen that the maximum force of 10.66kN/m is required for the implementation of the device.

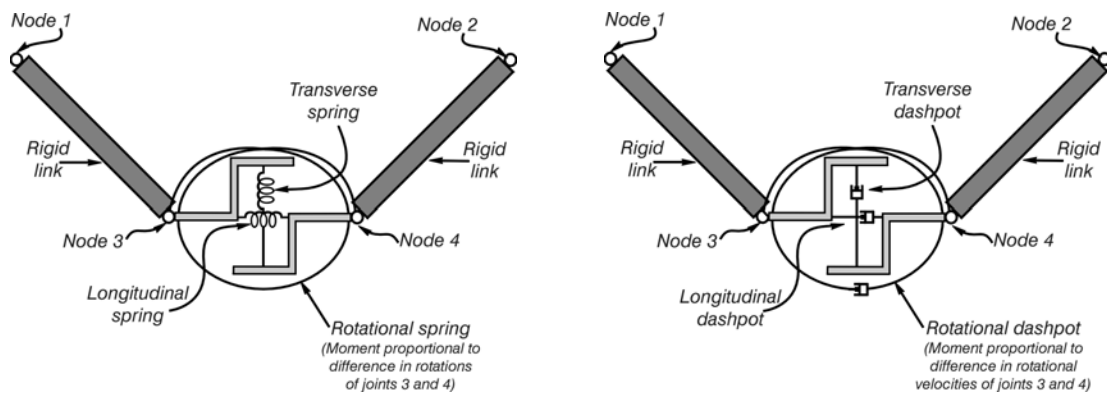


Figure 4. Spring and Damper Member (Ruaumoko 2D)

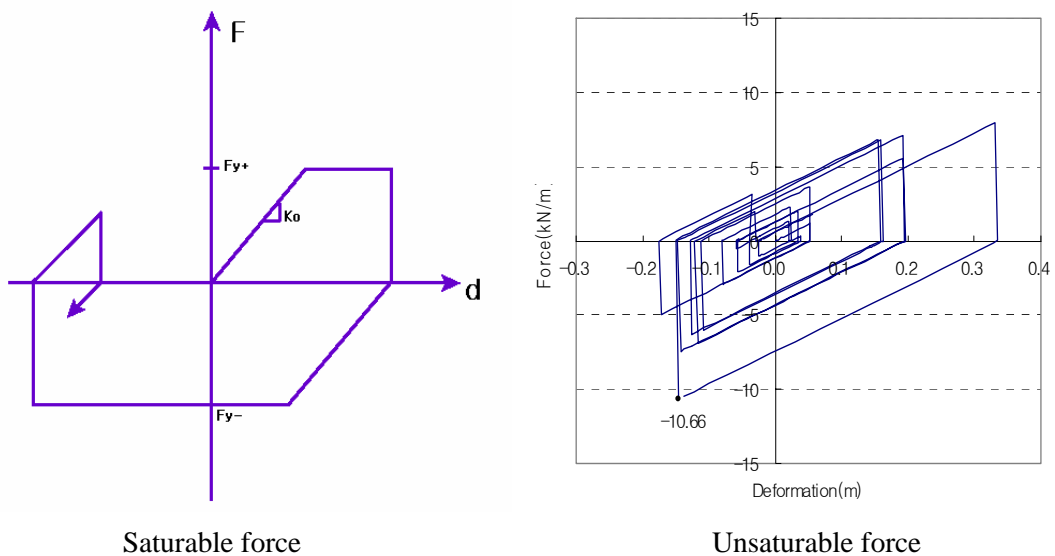


Figure 5. Hysteresis behavior of Resettable Device (saturable and unsaturable force cases)

3.3. 2DOF model implementation

In order to demonstrate the proposed structural control methodology, 2DOF linear undamped model is studied. In the parametric point of view, the optimal frequency tuning ratio, f_{2opt} and damping ratio, ξ_{2opt} are adopted from the equation of Sadek et al. and also, the practical optimal parameters of SATMD stiffness, k_{2opt} , and damping coefficient, c_{2opt} , are calculated. While, the SATMD stiffness, k_{2opt} , is composed by resettable device stiffness and rubber bearing stiffness. To assess how much the resettable device stiffness is comparably beneficial, the percentage allocations of the resettable device stiffness to the total stiffness including the rubber bearing stiffness, were selected as 20%, 40%, 60%, 80% and 100%. To investigate the efficiencies of these five cases, the performances of No TMD, PTMD (Passive Tuned Mass Damper) are compared as shown in Table 2, and Figure 6 and 7.

The SATMD building system described above was investigated when both the SATMD and the main building are considered to be linear elastic. To observe the seismic responses under typical design based earthquake record, the El Centro NS earthquake event was used in the numerical simulations. This record has magnitudes of 6.4 on the Richter scale, and the accelerographs were recorded at sites 9 km from the epicenters and have PGA of 0.34g. The El Centro accelerogram has been used all over the world as the basis for design response spectra.

From the perspective of the practical implementation of structural control scheme, the maximum values of the required control force is important operational parameters. From the time histories of SA device force, it can be seen that the maximum required force of each device is depend on the stiffness of the resettable actuator device. For 2DOF model, the unsaturable force of 15kN/m was selected as a SA device force.

In order to illustrate the performance of each control case using the calculated optimal parameters, the root-mean square (RMS) and peak responses of the main system and the PTMD and SATMD strokes are computed as functions of mass ratio in Table 2. All the response values are normalized by uncontrolled responses and the stroke values are normalized by PTMD stroke responses. From the results in Table 2 and Figure 6 and 7, it is observed that all control cases perform much better than the uncontrolled system. It is also clear that the control effectiveness is generally better for RMS responses as opposed to peak responses. For example, the PTMD system and the five cases of the SATMD systems reduced the RMS displacements and RMS accelerations by more than 65% and 50% respectively. The PTMD system showed better reductions in responses of displacement and acceleration when compared with the SATMD systems, however, the PTMD control showed a two times larger stroke value compared to the SATMD cases. Due to the above stroke problem, the PTMD system is seen to as not a suitable TMD concept for large mass ratio. All the SATMD control cases perform almost similarly in displacement response reductions, except for strokes.

The SA40TMD (40% SA device stiffness to total stiffness) case is capable of providing better stroke reductions than any other SATMD control systems. Larger stiffness of the SA device increases the acceleration responses. This tendency is due to the application of the SA device, introducing a step change in forces when the control valve is switched on and off. Figure 8 and Figure 9 show the time histories of the relative displacement, the stroke and the total acceleration of the main system for SA40TMD case, respectively. It is observed that the system can reduce the response of the main system clearly. The time history of SA device force is displayed in Figure 10. The maximum force required for each control case is comparable varying from 6.85kN/m to 14.46kN/m.

TMD Type	Disp. (RMS)	>%	Disp. (Max)	>%	Stroke (RMS)	>%	Stroke (Max)	>%	Accel. (RMS)	>%	Accel. (Max)	>%
No TMD	0.174	100.0	0.317	100.0	0.006		0.011		1.51	100.0	2.70	100.0
PTMD	0.050	28.8	0.178	56.3	0.062	100.0	0.198	100.0	0.46	30.2	1.61	59.8
SA20TMD	0.056	32.5	0.154	48.7	0.042	67.7	0.117	59.4	0.60	39.5	1.76	65.2
SA40TMD	0.059	34.2	0.150	47.4	0.036	59.0	0.112	56.5	0.72	47.4	1.76	65.3
SA60TMD	0.060	34.7	0.150	47.5	0.035	56.1	0.090	45.5	0.78	51.3	2.10	77.8
SA80TMD	0.060	34.8	0.152	48.1	0.036	58.8	0.106	53.5	0.70	46.2	1.87	69.3
SA100TMD	0.060	34.3	0.152	48.2	0.037	60.8	0.122	61.6	0.77	51.0	2.24	82.9

Table 2. Response results for 2DOF model

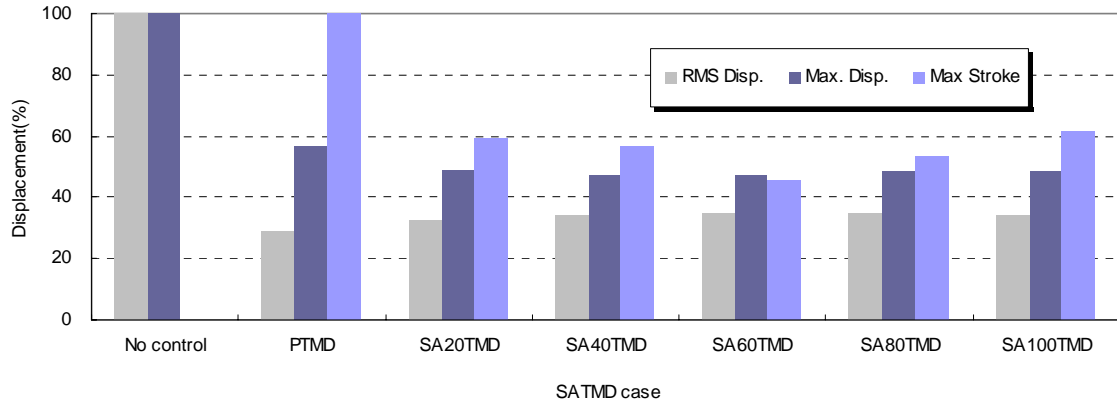


Figure 6. Comparison of displacement response reductions for PTMD and SATMDs

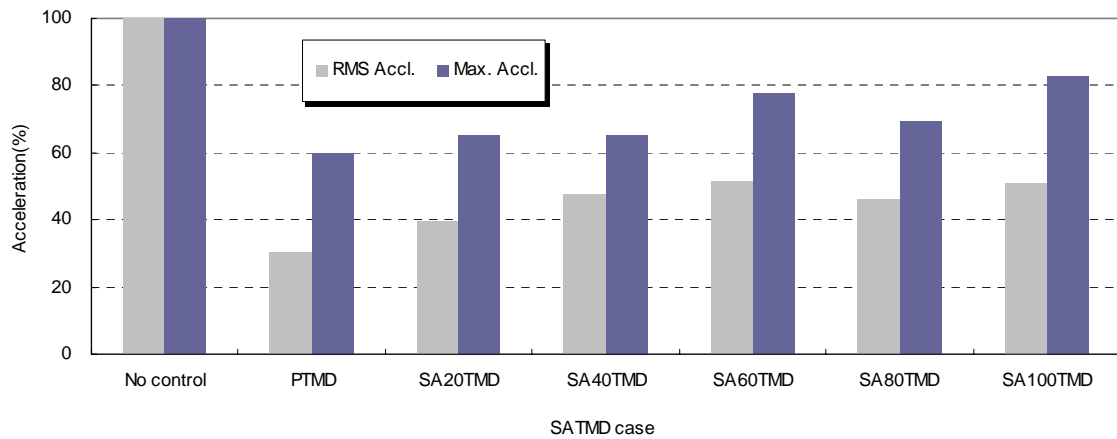


Figure 7. Comparison of acceleration response reductions for PTMD and SATMDs

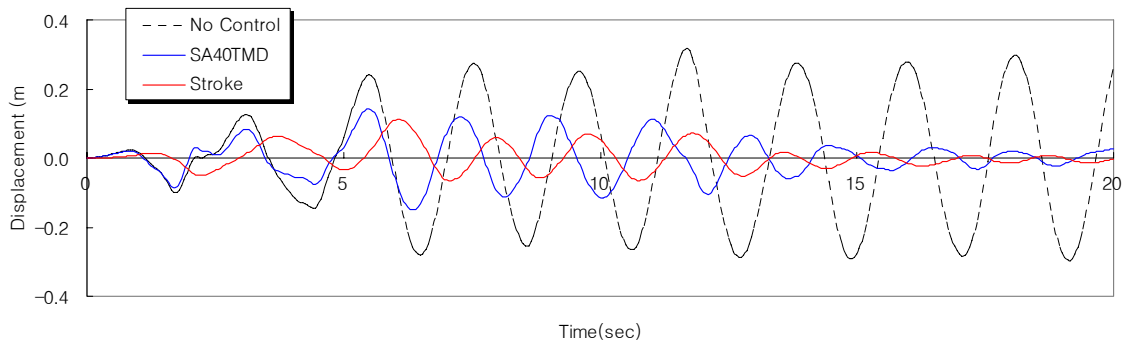


Figure 8. Displacement time history for SA40TMD

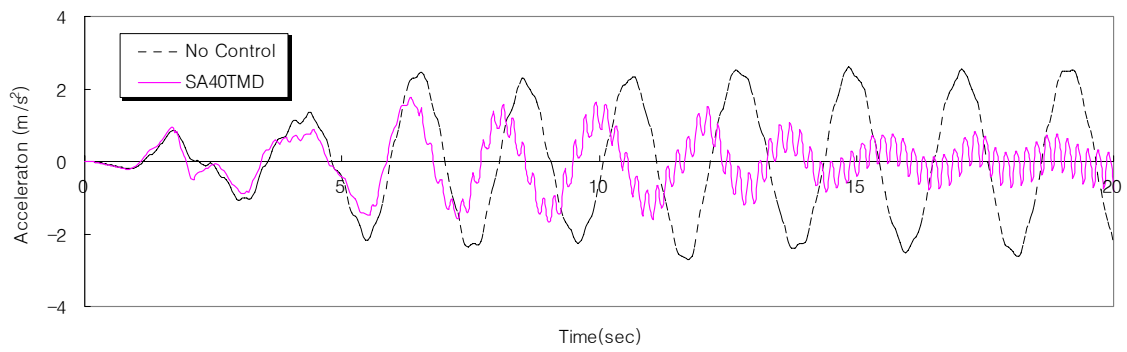


Figure 9. Acceleration time history for SA40TMD

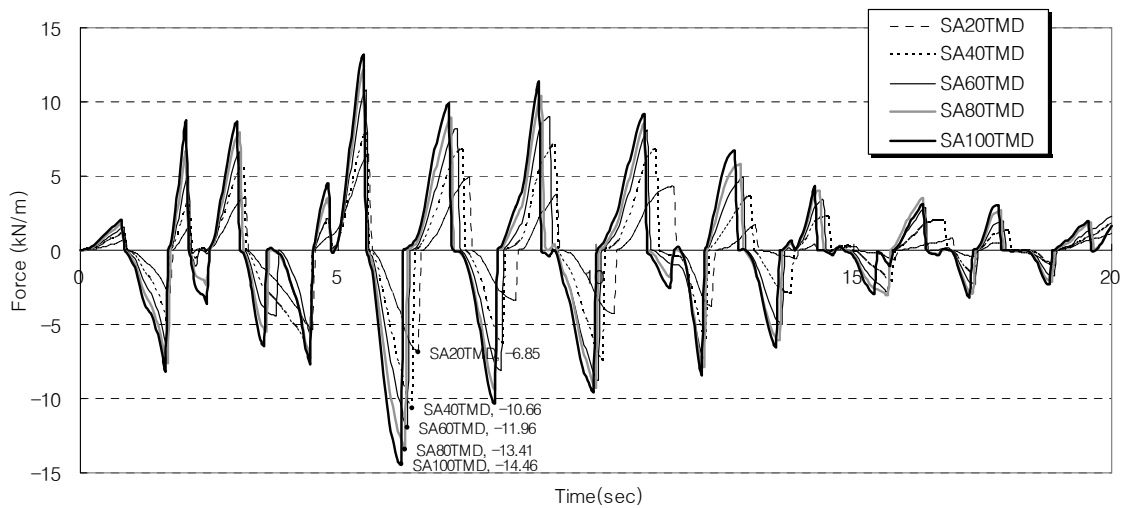


Figure 10. Device force time histories for SATMDs

4. BENCHMARK CASE STUDY (6 & 12 STORY MODEL)

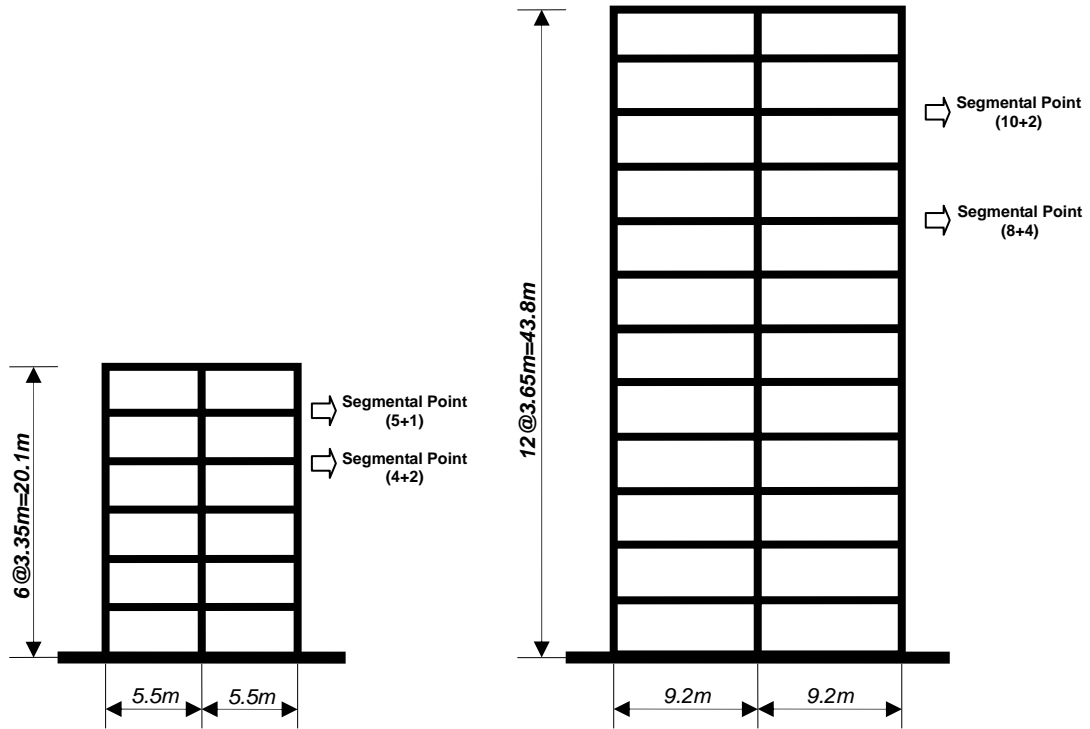


Figure 11. Modeling of 6 and 12-Story Two-Bay Reinforced Concrete Frame

Model	Nat. Period (sec)	1 st Mod. Mass (kN-s ² /m)	Mass Ratio	Tuning Ratio	Damping Ratio
6 Story	0.790	235	-	-	-
5(+1) Story	0.655	203	0.159	0.847	0.413
4(+2) Story	0.520	168	0.399	0.696	0.570
12 Story	1.880	1514	-	-	-
10(+2) Story	1.518	1301	0.164	0.843	0.418
8(+4) Story	1.187	1072	0.412	0.689	0.576

Table 3. Dynamic properties for 6 and 12 story building and optimum SATMD parameters

4.1. Structures and modeling

Six and twelve story, two-bay reinforced concrete framed structures have been developed in *RUAUMOKO 2D* to demonstrate the effects of the SATMD. The each model, shown in Figure 11, has a natural period of 0.79sec(1.27Hz) and 1.88sec(0.53Hz) respectively, and the damping ratio of the each model is assumed to be 5% of critical damping. The dynamic properties of the frame, such as the natural frequency and modal effective mass and optimal parameters are calculated and listed in Table 3. It was noted that under the considered structural properties and the ground excitations, the displacement response due to the first mode constitutes approximately 80%~90% of the total displacement response. Thus, the first mode was selected for the designs of the SATMD system. For the control of the 6-story model, a top story and upper two stories are used for the SATMD system, and for the 12-story model, upper two and four stories are used, respectively. The total value of k_{2opt} is allocated to rubber bearing stiffness and the stiffness of the SA device. Also, the SA acuator force is considered in the view point of the reasonable and saturable forces and the optimal parametric values are obtained from the Sadek's equations.

4.2. Performance results

The analytical results for the described buildings are obtained in order to check the performance of each structural control case. The performances are evaluated against the set evaluation criteria for both buildings (6 and 12 story) subjected to El Centro NS earthquake records. To investigate the efficacy of the SATMD building system compared to no control and passive

control system, the responses of No TMD, PTMD, and SATMD systems are compared in all floors.

To represent this, the numerical results are presented in Table 4 and 5. The response reduction factors for RMS and peak floor displacement are calculated from the floor displacement relative to the ground of the controlled system divided by the corresponding uncontrolled floor displacement. The response reduction factors for RMS and peak floor acceleration ratios are also calculated from the absolute floor acceleration of the controlled system divided by the corresponding uncontrolled floor acceleration. These evaluation criteria are all non-dimensional measures, and smaller values are associated with a more effective control system, so if the response reduction factors are less than 1.0, they indicate the increased ability of the control system to dissipate energy. In addition, the relative displacements between upper portion (SATMD) and lower portion (main system), the strokes, are calculated and presented. Meanwhile, '5+1' and '4+2' mean that the top and upper two stories are isolated for the control of 6 story model, and '10+2' and '8+4' mean that the upper two and four stories are isolated for 12 story structure, respectively.

From the results in Table 4 and 5, we investigate the control effectiveness in terms of the reduction it brings about in various floor and story responses. The SA operation of the SATMD clearly reduces most of the response quantities. However, the reduction in the peak acceleration responses for the 6-story structure is slightly increased. It is also clear that the response reduction for RMS response is almost better than peak response. Even though PTMD control cases still show good reductions in the responses generally, the most of the deformation of the building concentrates in the segmental point and this is a same practical problem as mentioned above the case of 2DOF model.

For the 6-story building, the SATMD (4+2) produced better reduction results than the SATMD

(5+1) in almost response criteria and this reflects on the advantage of larger mass ratio. The SATMD(4+2) reduced by 56%, 57%, 59%, 62%, 60%, and 60% for the RMS displacement response and by 41%, 42%, 45%, 50%, 30%, and 33% for peak displacement response, respectively, for 1st floor to 6th floor. However, the peak acceleration response for 6-story building is increased, except for the top story. For the 12-story building, both control cases, SATMD (10+2) and SATMD (8+4), produce better response reduction than 6-story building for all control criteria. The SATMD(8+4) response reduction factor for displacement response is less than the SATMD(10+2) one, however, the response reduction factor for acceleration response is larger than the SATMD(10+2).

The positive side peak relative displacements of each floor with respect to the ground for the two building models are shown in Figure 12. For comparison, the corresponding results of the No TMD and PTMD results are also shown in Figure 12. The SATMD(4+2) and SATMD(8+4) cases produced better performance reduction results than the SATMD(5+1) and SATMD(10+2) cases, respectively. Inter-story drift ratio results for the 6 and 12 story buildings are given in Figure 13. The SATMD(4+2) and SATMD(8+4) are generally more effective than the SATMD(5+1) and SATMD(10+2) respectively, however, there are still some large drift demands at lower stories for the SATMD(8+4) and at 7~8 stories for the SATMD(10+2) building.

Floor	Displacement(RMS)					Displacement(Max)					Acceleration(RMS)					Acceleration(Max)				
	No TMD (m)	TMD (5+1)	SATMD (5+1)	TMD (4+2)	SATMD (4+2)	No TMD (m)	TMD (5+1)	SATMD (5+1)	TMD (4+2)	SATMD (4+2)	No TMD (gal)	TMD (5+1)	SATMD (5+1)	TMD (4+2)	SATMD (4+2)	No TMD (gal)	TMD (5+1)	SATMD (5+1)	TMD (4+2)	SATMD (4+2)
6	0.035	0.83	0.48	0.65	0.40	0.114	0.88	0.61	0.67	0.57	2.37	0.58	0.48	0.46	0.50	9.13	0.64	0.56	0.58	0.72
5	0.032	0.48	0.58	0.68	0.40	0.103	0.69	0.81	0.70	0.56	2.04	0.65	0.85	0.48	0.51	7.24	0.98	1.18	0.55	0.76
4	0.026	0.50	0.61	0.40	0.38	0.084	0.72	0.85	0.50	0.63	1.73	0.63	0.85	0.58	0.71	5.39	1.09	1.31	0.92	1.12
3	0.019	0.51	0.63	0.42	0.41	0.061	0.72	0.86	0.55	0.71	1.45	0.65	0.84	0.57	0.70	4.87	1.01	1.16	0.91	1.14
2	0.013	0.52	0.65	0.43	0.43	0.039	0.73	0.87	0.58	0.76	1.18	0.72	0.85	0.65	0.75	4.30	1.05	1.25	0.93	1.05
1	0.006	0.52	0.66	0.44	0.44	0.018	0.74	0.88	0.59	0.79	0.81	0.89	0.94	0.86	0.91	3.06	1.11	1.14	1.15	1.24
Stroke(m)		0.076 0.045 0.044 0.030																		

Table 4. Response reduction factors for 6-story building

Floor	Displacement(RMS)					Displacement(Max)					Acceleration(RMS)					Acceleration(Max)				
	No TMD (m)	TMD (10+2)	SATMD (10+2)	TMD (8+4)	SATMD (8+4)	No TMD (m)	TMD (10+2)	SATMD (10+2)	TMD (8+4)	SATMD (8+4)	No TMD (gal)	TMD (10+2)	SATMD (10+2)	TMD (8+4)	SATMD (8+4)	No TMD (gal)	TMD (10+2)	SATMD (10+2)	TMD (8+4)	SATMD (8+4)
12	0.091	0.77	0.39	0.63	0.36	0.202	1.21	0.72	1.02	0.58	1.59	0.37	0.30	0.41	0.38	5.47	0.39	0.36	0.46	0.47
11	0.086	0.79	0.40	0.65	0.37	0.190	1.26	0.74	1.05	0.59	1.33	0.43	0.37	0.41	0.46	3.53	0.60	0.56	0.61	0.74
10	0.080	0.46	0.47	0.67	0.37	0.177	0.80	0.66	1.08	0.61	1.09	0.93	0.44	0.44	0.56	3.04	1.68	0.65	0.58	0.85
9	0.073	0.47	0.49	0.70	0.38	0.167	0.79	0.66	1.07	0.60	0.95	0.84	0.51	0.51	0.64	2.66	1.45	0.74	0.80	0.98
8	0.065	0.48	0.51	0.43	0.38	0.155	0.75	0.63	0.68	0.51	0.96	0.70	0.51	0.91	0.63	2.65	0.95	0.74	1.36	0.98
7	0.057	0.48	0.52	0.45	0.40	0.141	0.72	0.61	0.68	0.51	1.05	0.60	0.46	0.69	0.58	3.12	1.04	0.63	1.06	0.83
6	0.049	0.49	0.52	0.45	0.41	0.125	0.69	0.59	0.66	0.51	1.12	0.58	0.43	0.58	0.54	4.02	0.60	0.49	0.73	0.65
5	0.041	0.49	0.53	0.46	0.42	0.108	0.65	0.57	0.65	0.52	1.14	0.61	0.43	0.55	0.53	4.18	0.65	0.47	0.59	0.62
4	0.033	0.49	0.53	0.46	0.42	0.088	0.62	0.56	0.65	0.54	1.10	0.67	0.44	0.57	0.55	3.97	0.80	0.50	0.64	0.65
3	0.024	0.49	0.54	0.46	0.43	0.066	0.60	0.55	0.66	0.56	1.00	0.74	0.48	0.65	0.61	3.74	0.91	0.52	0.73	0.69
2	0.015	0.50	0.54	0.46	0.43	0.042	0.59	0.56	0.67	0.58	0.87	0.83	0.56	0.79	0.70	2.99	1.08	0.66	0.93	0.87
1	0.007	0.50	0.55	0.46	0.43	0.018	0.60	0.57	0.68	0.59	0.71	0.94	0.68	0.92	0.85	3.00	1.07	0.66	1.03	0.87
Stroke(m)		0.190 0.111 0.126 0.078																		

Table 5. Response reduction factors for 12-story building

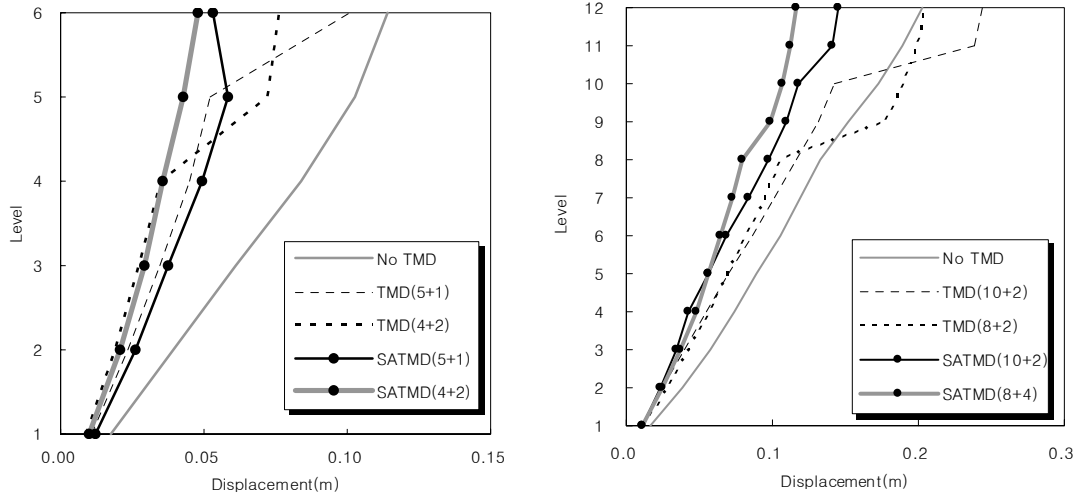


Figure 12. Maximum relative displacements for 6 and 12 story building

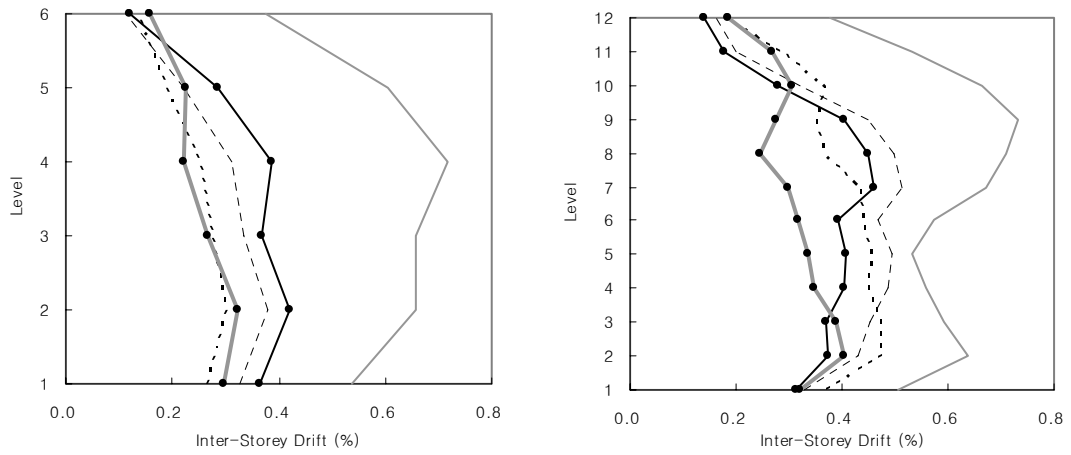


Figure 13. Maximum inter-story drift ratios for 6 and 12 story building

5. CONCLUSIONS

Multi Story Semi-Active Tuned Mass Damper Building System has been proposed through numerical simulation. For the large mass ratio due to the building's upper story(s), Sadek et al's equations have been used to find the optimal parameters of tuning and damping ratio. A 2DOF undamped model has been used to explore the efficiency of parametric control, and for the case studies, 6 and 12-stories, two-bay reinforced concrete framed structures have been developed in RUAUMOKO to demonstrate the effects of the SATMD under El Centro NS records. The total value of k_{2opt} was allocated to rubber bearing stiffness and the stiffness of the SA device and the optimal damping ratio, c_{2opt} , has been incorporated in analysis.

The performances of No TMD, PTMD, and SATMD systems have been observed and compared. The PTMD produced good reductions of the RMS displacements and accelerations, however, the PTMD produced relatively large strokes compared to SATMD cases. The SA operation of the SATMD clearly reduces most of the response quantities. All the SATMD cases produced almost similarly in displacement response reductions, except for strokes. The larger stiffness of SA device increased the acceleration responses due to the application of SA device. The maximum values of the required control force have been investigated and adopted.

For the 6-story building, simulation results indicate that performance of SATMD is superior to that of the uncontrolled structure in reducing the almost response criteria. However, the peak acceleration response for the 6-story building is increased, except for the top story. The SATMD(4+2) produced better reduction results than the SATMD(5+1) in almost response criteria and this reflects on the advantage of larger mass ratio. For the 12-story building, both control cases, SATMD (10+2) and SATMD (8+4), produce better response reduction than 6-story building for all control criteria. The SATMD(8+4) response reduction factor for

displacement response is less than the SATMD(10+2) one. However, the response reduction factor for acceleration response is larger than the SATMD(10+2). The responses of inter-story drifts and peak relative displacements of multi story SATMD building system also represent the positive role of the large mass ratios.

APPENDIX. NOTATION

x_1	absolute displacement of main system
x_2	absolute displacement of PTMD or SATMD
y_1	relative displacement between the main system and the ground
y_2	relative displacement between the PTMD or SATMD and the main system
\ddot{x}_1	absolute acceleration of the main system
\ddot{x}_2	absolute acceleration of the PTMD or SATMD
x_g	absolute displacement of ground
m_1	mass of main system
m_2	mass of PTMD or SATMD
μ	mass ratio of the PTMD or SATMD to the main system
f_2	frequency tuning ratio of the PTMD or SATMD to the main system
ξ_1	damping ratio of the main system
ξ_2	damping ratio of the PTMD or SATMD
k_1	stiffness of main system
k_{act}	effective stiffness of resettable actuator
k_{RB}	effective stiffness of rubber bearing
k_2	combined stiffness of resettable device and rubber bearing
c_1	damping coefficient of main system
c_2	damping coefficient of PTMD or SATMD
u	control force of resettable actuator
ω_1	frequency of the main system
ω_2	frequency of the PTMD or SATMD
Φ	amplitude of the mode shape at the PTMD location
U_{act}	energy in a single resettable actuator,
F_{max}	resettable actuator saturation force
v	relative displacement of the resettable actuator end
v_0	free length of the resettable actuator pneumatic spring
\dot{v}	relative velocity of the actuator ends
opt	optimum value corresponding to the parameters
SA	semi-active
2DOF	two-degree of freedom
TMD	tuned mass damper
PTMD	passive tuned mass damper
SATMD	semi-active tuned mass damper
RMS	root-mean-square

REFERENCES

1. Abe M. Semi-active tuned mass dampers for seismic protection of civil structures. *Earthquake Engineering and Structural Dynamics* 1996; **25**:743-749.
2. Barroso LB., Chase JG., Hunt S. Resettable smart dampers for multi-level seismic hazard mitigation of steel moment frames. *Journal of Structural Control* 2003; **10**: 41-58.
3. Carr AJ. RUAUMOKO. Computer Program Library, Department of Civil Engineering, University of Canterbury, 2004.
4. Chey MH. Parametric control of structures using a tuned mass damper system under earthquake excitations. ME Thesis, Department of Civil Engineering, University of Canterbury, Christchurch, New Zealand, 2000.
5. Djajakesukma SL., Smali B., Nguyen H. Study of a semi-active stiffness damper under various earthquake inputs. *Earthquake Engineering and Structural Dynamics* 2002; **31**:1757-1776.
6. Feng MQ, Mita A. Vibration control of tall buildings using mega subconfiguration. *Journal of Engineering Mechanics* 1995; **121**(10):1082-1088.
7. Hrovat D., Barak P., Rabins M. Semi-active versus passive or active tuned mass dampers for structural control. *Journal of Engineering Mechanics* 1982; **109**(3): 691-705.
8. Hunt S J. Semi-active smart-dampers and resettable actuators for multi-level seismic hazard mitigation of steel moment resisting frames. ME Thesis, Department of Civil Engineering, University of Canterbury, Christchurch, New Zealand, 2002.
9. Jabbari F., Bobrow JE. Vibration suppression with resettable device. *Journal of Engineering Mechanics* 2002; **128**(9):919-924.
10. Jagadish KS., Prasa B K R., Rao PV. The inelastic vibration absorber subjected to earthquake ground motions. *Earthquake Engineering and Structural Dynamics* 1979; **7**:1317-326.
11. Murakami K., Kitamura H., Ozaki, H., Teramoto T. Design and analysis of a building with the middle-story isolation structural system. *12th World Conference of Earthquake Engineering* 2000; **0857**:1-8.
12. Miranda JC. On tuned mass dampers for reducing the seismic response of structures. *Earthquake Engineering and Structural Dynamics* (in press).
13. Miyama T. Seismic response of multi-story frames equipped with energy absorbing story on its top. *10th World Conference of Earthquake Engineering* 1992; 4201-4206.
14. Pan TC., Cui W. Response of segmental buildings to random seismic motions. *ASET Journal of Engineering Technology* 1998; Paper No. 378, **35**(4):105-112.
15. Pan TC., Ling SF., Cui W. Seismic response of segmental buildings. *Earthquake Engineering and Structural Dynamics* 1995; **24**:1039-1048.
16. Sadek F., Mohraz B., Taylor AW., Chung RM. A method of estimating the parameters of tuned mass dampers for seismic applications. *Earthquake Engineering and Structural Dynamics* 1997; **26**:617-635.
17. Villaverde R. Seismic roof isolation system: Feasibility study with 13-story building. *Journal of Structural Engineering* 2002; **128**(2):188-196.
18. Villaverde R. Reduction in seismic response with heavily-damped vibration absorbers. *Earthquake Engineering and Structural Dynamics* 1985; **13**:33-42.
19. Yang JN., Agrawal AK. Semi-active hybrid control systems for nonlinear buildings against near-field earthquakes. *Engineering Mechanics* 2002; **24**:271-280.
20. Yang JN., Kim JH., Agrawal AK. Resetting semiactive stiffness damper for seismic response control. *Journal of Structural Engineering* 2000; **126**(12):1427-1433.